Simulation of Print Quality Defects

Woonyoung Jang and Jan P. Allebach
School of Electrical and Computer Engineering
Purdue University
West Lafayette, IN 47907-1285

Abstract

The simulation of print quality (PQ) defects is a process in which an image is degraded by artificially generated structures to create an impression of real defects when the image is viewed or printed. The simulation algorithms generate a set of defective images that can be used in diagnostic tools for printer users. These algorithms can also provide experimental images for psychophysical evaluations regarding defect perception, which requires the capability to control the level of the defects. In addition, simulation of defects aids in testing the usability of a PQ assessment page, and the development of computer algorithms for detecting PQ defects. Thus there are many applications that need high quality simulation of PQ defects. However, little research has been devoted to this work. In this paper, we characterize the common PQ defects in color laser printers such as banding, streaks, ghosting, and repetitive artifacts. We classify these defects into three categories: defects of uniformity, defects of random marks or repetitive artifacts, and color defects. We develop a simulation model for each defect based on its features such as the shape and the spatial distribution of the defect marks, or the tone dependency of the defect. The defects are simulated on RGB color continuous-tone images.

1. Introduction

Print quality(PQ) defects of laser printers are the artifacts degrading the quality of printed images, which are generated by the electrophotographic process and/or print mechanism.

PQ defects can be caused by the non-ideal characteristics of printer units, or by physical damage to them. The defects may be categorized into three groups: 1) defects of uniformity, 2) random marks or repetitive artifacts, and 3) color defects. The defects in the first group produce visible density variations appearing as banding or streaks in constant tone areas. The second group has two different types: one is random and the other is repetitive. The former gives an appearance of randomly distributed dots or smudges, while the latter shows repetitive marks with a fixed interval. The third group includes the problem of temporal color inconsistency and the failure of color plane registra-tion. In this paper, we will discuss simulation methods for the first two defect groups.

Although considerable research has been devoted to analyzing many types of PQ defects such as banding,[1, 2, 3, 4, 5, 6] streaks,[4, 6, 7] and ghosting,[8, 9] little attention has been paid to simulating those defects. In this paper, we characterize the common PQ defects in color laser printers. Based on the characterization and measurement of each defect, we describe a simulation procedure for adding the defect to continuous-tone images.

The rest of the paper is organized as follows. In Sec. 2, we describe a general framework for simulation of PQ defects. Section 3 discusses how to simulate defects of uniformity by using tone dependency functions. In Sec. 4, we show simulation methods for the defects of random marks and repetitive artifacts.

In this paper, we will use the letters C, M, Y, and K for denoting the colors of cyan, magenta, yellow, and black, respectively.

2. General Framework for Simulation of PQ Defects

To simulate a defect in a continuous-tone image, we perform the following steps. First, we characterize the defect by measuring its features such as the shape and the spatial distribution of the defect marks, or tone dependency of the defect. We measure the features by scanning defective prints. In our work, we used a flatbed scanner (Heidelberg Saphir Ultra2: Heidelberg USA, Inc., Kennesaw, GA30144) and converted the scanner values to absorptance values via a scanner calibration curve. We then build a simulation model for the defect based on the measurements. The model specifies a simulation procedure which

shows how to synthesize the defect within a continuous-tone image. The block diagram in Fig. 1 depicts the general framework of the simulation procedure, which is common to all the defects described in this paper.

The input to this simulation process is an RGB continuous-tone image, which is converted into a CMY continuous-tone image. Since the simulation methods described in this paper are not specific to a particular printer, we use
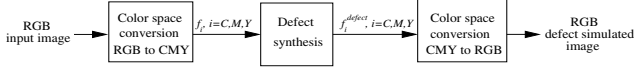
Figure 1: *General framework for simulation of PQ defects. This procedure is common to all the defects described in this paper.*

the simple transformation from RGB space to CMY space given by

$$[C\ M\ Y]^t = [1\ 1\ 1]^t - [R\ G\ B]^t, \qquad (1)$$

where $0 \leq R \leq 1$, $0 \leq G \leq 1$, and $0 \leq B \leq 1$. We can easily replace this by the transformation for a particular printer if this is desired. After the color space conversion, we separately synthesize the defect features for the CMY color planes. Finally we convert back to RGB.

In this paper, we will use the term *normalized digital value* to indicate the CMY color value $a_i \in [0, 1]$, $i = C, M, Y$.

3. Simulation of Defects of Uniformity

The defects of uniformity are print artifacts that are easily noticed in nominally uniform areas. In this section, we will show how to simulate banding and streaks, which are very common defects of laser printers.

3.1. Banding

In an electrophotographic laser printer, a laser beam is scanned across the surface of an optical photoconductor (OPC) drum in a direction perpendicular to the motion of the OPC drum. Since the velocity of the OPC drum generally varies with time, its vibratory motion causes the raster lines on the surface of the drum to be unevenly spaced [3,5]. These raster position errors result in density variation in the paper process direction, which appears as tightly packed lines.

Banding is more prominent at certain tone levels than at others. We developed a measurement method for characterizing this tone dependency. We obtain the Banding Tone Dependency Function (BTDF) by the following steps.

1. A test target page consisting of solid bars at twenty different normalized digital values (a=0.05, 0.10, 0.15, ..., 1.00) is generated and saved in TIFF file format. The size of each bar is 5.4 in × 0.5 in.

2. We print ten test target pages from a laser printer using the printer driver's halftoning technique.

3. We scan the printed test target pages at 600 dpi, and crop each test bar to avoid edge effects. We then convert the scanner values to absorptance values by using a scanner calibration curve.

4. For a given tone a, we obtain the 1D segment $g_a^{(l)}[n]$ by averaging each column of scanned data $g_a^{(l)}[m, n]$

perpendicular to the paper process direction as

$$g_a^{(l)}[n] = \frac{1}{M} \sum_{m=1}^{M} g_a^{(l)}[m, n], \qquad (2)$$

where M is the number of points per segment perpendicular to the paper process direction, and l is the bar index which represents the test target page number out of ten pages in this measurement. We call this segment the *projected absorptance profile*.

5. From $g_a^{(l)}[n]$, we compute a periodogram[10] as

$$P_a^{(l)}(v) = \frac{1}{N} \left| \sum_{n=0}^{N-1} g_a^{(l)}[n] e^{-j2\pi vn/R} \right|^2, \qquad (3)$$

where N is the number of points per segment, and l is the segment index. Then we obtain a power spectrum estimate $S_a(v)$ by using Bartlett's method[10], which averages the periodograms for L segments as

$$S_a(v) = \frac{1}{L} \sum_{l=1}^{L} P_a^{(l)}(v). \qquad (4)$$

6. For a given tone a, we calculate the power $E(a)$ from the power spectrum estimate $S_a(v)$ over a certain frequency range which is considered to be associated with banding.

7. The *spline* function in MATLAB yields the interpolated curve $\hat{E}(a)$ from the measured data points $E(a), a = 0.05, 0.10, ..., 1.00$.

8. Normalizing the square root of $\hat{E}(a)$ yields the BTDF

$$h^b(a) = \frac{\sqrt{\hat{E}(a)}}{\max_{0 \leq a \leq 1} \sqrt{\hat{E}(a)}}, a \in [0, 1]. \qquad (5)$$

In our experiment, we calculated the power for the frequency range [5, 90] cycles/in which contains most of the major banding frequencies, and used that power to obtain a tone dependency function. The resulting BTDF for the K plane is shown in Fig. 2(a).

By utilizing the BTDF obtained above, we build a banding simulation model for a monochrome image as

$$f^{\text{defect}}[m, n] = f[m, n] + \rho h(f[m, n])d[n], \qquad (6)$$

where $f[m, n]$ is the input image, ρ is a parameter controlling the overall defect level, $h(\cdot)$ is the tone dependency function, and $d[n]$ is a prototype defect signal weighted by the tone dependency function.

The banding signal is generated by using a sample projected absorptance profile, and processing it to retain the frequency range which is considered to be associated with banding. We utilize an ideal bandpass filter which has unit magnitude response in this interval and zero response elsewhere. The passband of the filter that we used is [5, 90]
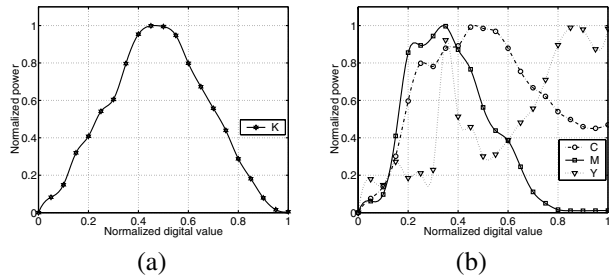
(a)   *(b)*

Figure 2: *Measurement of banding tone dependency for (a) K plane, and (b) CMY planes. The ratio of the maximum power for these color planes is K:C:M:Y = 1 : 0.80 : 0.87 : 0.29.*
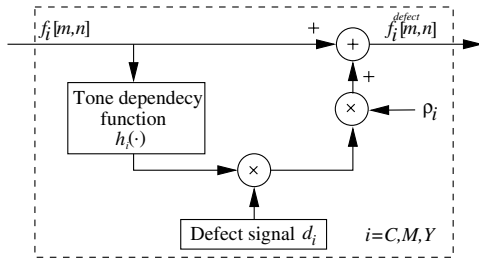

Figure 3: *Defect synthesis block for banding and streaks in a color image.*

cycles/in, which is the same frequency range as used to obtain the BTDF. After the filtration process, we obtain a final banding signal by normalizing the bandpass filtered signal to have RMS value unity.

    We can extend this method to the banding simulation for color images by using separate BTDFs and banding signals for the CMY planes. The BTDFs and banding signals for the CMY planes are measured and obtained as described above. The resulting banding tone dependency for the CMY color planes is shown in Fig. 2(b).

    The general framework introduced in Fig. 1 is also used in the simulation of banding. Figure 3 shows the defect synthesis block in detail. The input to the block is a CMY color image. Each color plane is separately processed according to Eq. (6). The banding simulation result is shown in Fig. 4, where banding appears as closely spaced vertical lines.

3.2. Streaks

Streaks are another type of defect of uniformity that are easily observed in a constant tone area. Streaks are a unidirectional defect that can be characterized by a 1D additive signal[4, 6, 7] in a manner similar to that for banding. However, the appearance of streaks is different than that of banding. While banding appears as tightly packed periodic lines perpendicular to the paper process direction, the streak defect has rather irregular and wider lines in the paper process direction.

    The strength of the streak defect also depends on the tone level. Thus we consider the tone dependency of streaks

Figure 4: *Banding simulation image. Banding appears as closely spaced vertical lines.*

in the simulation process as we do in simulating the banding defect. We then model the streak simulation by using Eq. (6) with a slight change to the index of the defect signal. Since the direction of the streak defect is perpendicular to that of the banding defect, we use $d[m]$ instead of $d[n]$ for the streak simulation.

    We generate the streak signal in a way similar to that used to obtain the banding signal. We filter the projected absorptance profile to retain a frequency range which is considered to be associated with the streak defect. The frequency interval that we chose is [1, 35] cycles/in.
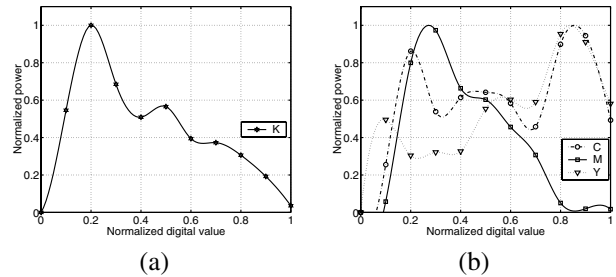

(a)   *(b)*

Figure 5: *Measurement of streak tone dependency for (a) K plane, and (b) CMY planes. The ratio of the maximum power for these color planes is K:C:M:Y = 1 : 0.74 : 1.97 : 0.18.*

    We incorporate the tone dependency of the streak into the simulation procedure by measuring the spectra of streaks at various tone levels and defining the STDF which plays the same role as does the BTDF in banding simulation. We obtain the STDF by following steps similar to those used to generate the BTDF. However, we note that the direction of the streak defect is perpendicular to that of the banding defect so the projected absorptance profiles are obtained in the perpendicular direction too. Figure 5(a) shows the streak tone dependency for the K plane measured at ten different tone levels.

    As was done with the banding simulation, we extend this method to streak simulation for color images by using separate STDFs and streak signals for the CMY planes.

Figure 6: *Streak simulation image. The streaks appear as irregular horizontal lines. Here the cyan plane was assumed to be defective in the simulation process.*
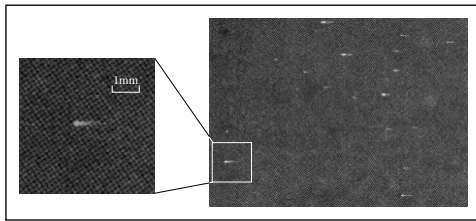

Figure 7: *Scanned sample of scattered white specks.*

The measured streak tone dependency for the CMY color planes is shown in Fig. 5(b). The defect synthesis block for streak simulation in a color input image is the same as that for the banding simulation shown in Fig. 3. A streak simulation image is shown in Fig. 6, where irregular horizontal lines appear.

4. Simulation of Random Marks or Repetitive Artifacts

The PQ defects described in the previous section are distributed over the entire image, and lack distinct boundaries. In this section, we will discuss defects that are rather localized. For some of them, the marks are randomly scattered across the page. Others appear in a repetitive pattern. We will present simulation procedures for three defects belonging to this second defect group: randomly scattered white specks, repetitive marks, and ghosting.

4.1. Randomly Scattered White Specks

Unwanted materials can be dispersed and built up on the OPC drum. Then toner particles cannot be developed at the positions where these contaminants occur. For a sequential architecture in which the same OPC drum is used for all four colorants, this problem will occur at the same position in all four color planes. As a result, scattered small white specks appear on the print as shown in Fig. 7.
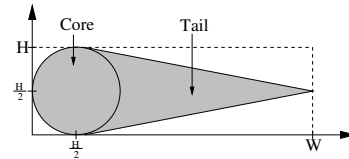

Figure 8: *Shape modeling of the white speck. This model consists of core and tail parts.*
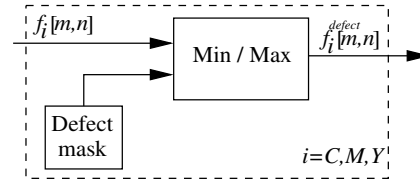

Figure 9: *Defect synthesis block for randomly scattered white specks and repetitive marks in a color image. The min operator is used for the former, and the max operator for the latter.*

We used a test target page which has a 100% black field of size 7 in $\times$ 10 in. We printed the test target page from a printer with a contaminated OPC drum. We scanned the printed test target page at 1200 dpi, and cropped it to 6 in $\times$ 9 in to retain only a black field area. The white specks in the scanned test target page were separately segmented.

We noticed that the white specks are horizontally elongated, and have a tail-like area which fades out. Based on this inspection, we model the white speck as shown in Fig. 8. According to this model, one white speck is generated by using two parameters, width W and height H.

In the scanned test target image, we segmented 589 white specks and measured their sizes. Then we statistically analyzed the data distributions of W and H. Based on the analysis, we modeled the width W by using a Gamma distribution. For a given W, we used a linear regression to find H by exploiting the relationship between the distribution of H and that of W. We also statistically analyzed and modeled the positions where the white specks are placed on the page. Based on the measured data, we used a Gaussian distribution for the vertical (process direction) position and a uniform distribution for the horizontal (scan direction) position.

Figure 9 demonstrates the defect synthesis block for randomly scattered white specks and repetitive marks. For each white speck, a pair of random parameters (W, H) for the size is generated based on the distributions described above. The shape of the white speck is then based on the model depicted in Fig. 8. The white speck is placed at a random position in the input image by setting the digital values of the corresponding pixels of the CMY planes to zeros. This can be done by using the *min* operator and a defect mask which has zeros on the position of the white specks and ones elsewhere. Figure 10 shows the resulting randomly scattered white specks in a continuous-tone

Figure 10: *Scattered white speck simulation image.*

Figure 11: *Samples of repetitive defect marks acquired from actual defective images.*

image.

4.2. Repetitive Marks

Repetitive marks are due to localized contamination or damage occurring on the surface of a drum or roller. Because of the contamination or damage, normal imaging cannot take place at this point on the surface of the drum or roller and a localized artifact results. This artifact repeats on the printed page in the process direction with a period given by the circumference of the drum or roller.

To generate a defect mark to be inserted in the input image, we segment defect marks from actual defect sample images. Then we use them in the simulation procedure.

Figure 11 shows the samples of defect marks, which are manually segmented from actual defect images. In the simulation procedure, a defect mark is separately put on each of the CMY color planes of an input image according to the repeating pattern by using the *max* operator and a defect mask as shown in Fig. 9. The black mark can be simulated by putting the same mark on all CMY planes at the same location. Figure 12 shows a simulation image containing repetitive CMYK defect marks in a row.

4.3. Ghosting

Ghosting is a PQ defect showing a dimly repeated image at an interval in the paper process direction. The source of ghosting is residual toner particles on the surface of a printer unit such as an OPC drum or a fuser[8, 9]. If a cleaning unit does not work properly, remaining toner particles from the previous image will be transferred onto the paper, thereby showing a ghost image.

We noticed that the ghosting image is more clearly visible when the tone of the source image is darker and when

Figure 12: *Repetitive defect simulation image. A pattern of defective marks in alternating colors repeats across the page in the horizontal (process) direction.*
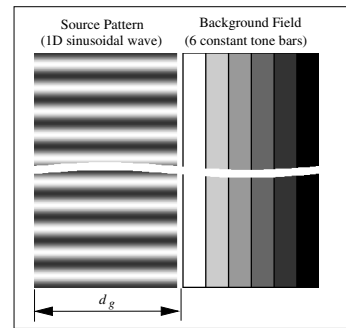

Figure 13: *The test target page used to measure ghosting tone dependency. When the page is printed with a defective printer, the source pattern will be dimly repeated on the background field showing ghosting at an interval d_g.*

the tone of the background where the ghosting shows up is lighter. This motivated us to study the tone dependency of ghosting. We developed a set of test target pages to quantify this phenomenon. A sample test target page is shown in Fig. 13. In our test target pages, we employed a sinusoidal waveform. We call this sinusoidal waveform which provokes the ghosting defect the *source pattern*. We also call the constant tone bar where ghosting appears the *background field*. We measured the ghosting tone dependency by examining how clearly the ghosting defect appears on the background fields at various tone levels while changing tone level of the source pattern.

Let a^b and a^s be the normalized digital value of the background field and the source pattern, respectively. We use six different tone levels for the background fields: $a^b = $ 0.0, 0.2, 0.4, 0.6, 0.8, and 1.0. For a given test target page, we fixed the amplitude and the bias of the source pattern signal as

$$s_{a^s}[m] = \frac{a^s}{2}\sin(2\pi v_g m/R) + \frac{a^s}{2}. \qquad (7)$$

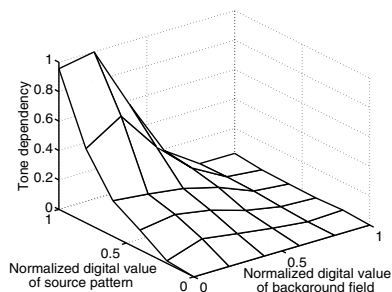We use five different tone levels of the source pattern: a^s

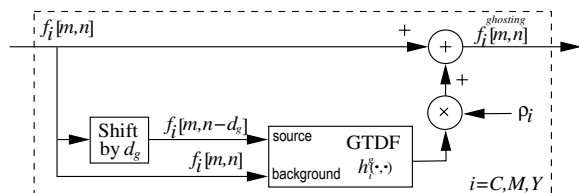*Figure 14*: *Measurement of ghosting tone dependency for the M plane*

Figure 15: *Ghosting synthesis block for a color image*

Figure 16: *Ghosting simulation image. The front part of the airplane is dimly repeated on the light tone area.*

References

1. P. W. Melnychuck, "Fourier spectra of digital halftone images containing dot-position errors," *Journal of Optical Society of America*, vol. 5, no. 8, pp. 1328–1338, 1988.
2. B. Mishra and D. R. Rasmussen, "Microuniformity: An image quality metric for measuring noise," pp. 75–78, *Proc. PICS*, 2000.
3. R. P. Loce, W. L. Lama, and M. S. Maltz, "Modeling vibration-induced halftone banding in a xerographic laser printer," *Journal of Electronic Imaging*, vol. 4(1), pp. 48–61, 1995.
4. P. J. Kane, T. F. Bouk, P. D. Burns, and A. D. Thompson, "Quantification of banding, streaking and grain in flat field images," pp. 79–83, *Proc. PICS*, 2000.
5. G.-Y. Lin, J. M.Grice, J. P. Allebach, and G. Chiu, "Banding artifact reduction in electrophotographic printers by using pulse width modulation," pp. 281–286, *Proc. NIP16*, 2000.
6. D. Rasmussen, E. N. Dalal, and K. M. Hoffman, "Measurement of macro-uniformity: Streaks, bands, mottle and chromatic variations," pp. 90–95, *Proc. PICS*, 2001.
7. H. Mizes, N. Goodman, and P. Butterfield, "The perceptibility of random streaking," pp. 89–93, *Proc. PICS*, 2000.
8. J. C. Briggs, E. Hong, and D. Forrest, "Analysis of ghosting in electrophotography," pp. 403–407, *Proc. NIP16*, 2000.
9. P. L. Jeran and N. Burningham, "Measurement of electrophotographic ghosting," pp. 80–83, *Proc. PICS*, 2001.
10. J. G. Proakis and D. G. Manolakis, *Digital Signal Processing*. Prentice Hall, third ed., 1996.

Acknowledgement

Biography

Woonyoung Jang received his BS and MS in electrical engineering from Korea University, South Korea in 1994 and 1996, respectively. He is now pursuing his PhD in the school of electrical and computer engineering at Purdue University. His fields of interest are print quality analysis, electronic imaging system, and color science.

= 0.2, 0.4, 0.6, 0.8, and 1.0. We set the frequency of the source pattern signal to v_g = 2 cycles/in.

To obtain the Ghosting Tone Dependency Function (GTDF), we first calculate the FFT magnitude at v_g for each pair (a^s, a^b) from the scanned test target page, and interpolate the data points. Then we normalize the interpolated data so that GTDF $h^g(a^s, a^b)$ has a maximum value of one.

Figure 14 shows the ghosting tone dependency for the M plane. As discussed earlier, the strength of ghosting increases with the absorptance of the source and decreases with the absorptance of the background.

By utilizing the GTDF, we devise a ghosting simulation model as

$$f_i^{\text{ghosting}}[m,n] = f_i[m,n] + \rho_i \cdot h^g{}_i(f_i[m,n-d_g], f[m,n])), \tag{8}$$

where d_g is the ghosting interval and ρ_i is the parameter controlling the defect level and $i = C, M$, and Y. Figure 15 illustrates the ghosting synthesis block of this model. A ghosting simulation image is shown in Fig. 16, where the front part of the airplane is dimly repeated on the light tone area.

5. Conclusion

We characterized some of the PQ defects which are common to color laser printers, and developed models to simulate them on continuous-tone color images. Although we modeled defects obtained from a specific printer, the measuring methods and modeling approaches are quite general and could be applied to defects from other types of printers, as well.